Rev. Roum. Sci. Techn.– Électrotechn. et Énerg.
Vol. **62**, *2*, pp. 148–153, Bucarest, 2017

PARTICLE SWARM OPTIMIZATION ALGORITHM-BASED FAULT LOCATION USING ASYNCHRONOUS DATA RECORDED AT BOTH SIDES OF TRANSMISSION LINE

MAHDI GHAZIZADEH-AHSAEE[1], MOSTAFA GHAZIZADEH-AHSAEE[2], NAJME GHANBARI[3]

Key words: Distributed parameter line model, Fault location, Non-synchronous voltage and current, Particle swarm optimization algorithm.

Recently, particle swarm optimization (PSO) has been lucratively applied to different problems of power system optimization. The accurate fault location problems which utilize the distributed parameter line model have complicated functions with inequality constraints that make the problem of finding the global optimum difficult utilizing any mathematical method. In this paper, fault location method based on the PSO is presented. In this method, asynchronous voltage and current data on both sides of transmission line is utilized, and the location of fault and the time required for data synchronization are calculated simultaneously by solving an optimization function, using the PSO algorithm. This method is executed based on the distributed parameter model of transmission line which fully considers the capacitance effect of the line. In addition, this algorithm is not dependent on the type of fault, the fault incidence angle, and the Thevenin equivalent impedances of both sides of the line. The proposed method has been evaluated using a variety of faults in various conditions and different fault incidence angles on the simulated network in MATLAB/Simulink. The results showed the high accuracy of the proposed method.

1. INTRODUCTION

The particle swarm optimization (PSO) has been recommended by [1] based on the similarity of swarm of bird and school of fish. The algorithm, which is based on a metaphor of group relations, explores a space by regulating the paths of moving particles in a multidimensional space [2, 3]. The main characteristics of the PSO algorithm are: simple idea, easy execution, robustness to control parameters, and efficiency in calculation compared with mathematical methods and other heuristic optimization methods [4].

PSO have been successfully employed for diverse problems of power system optimization such as power system stabilizer design [5], reactive power and voltage control [2], dynamic security border recognition [6], efficiency improvement of vector controlled surface mounted permanent magnet synchronous motor drive [7], and optimal var dispatch [8].

Accurate fault location methods reduce the operating costs of the system and increase the system reliability. In transmission lines, a small percentage of error in computations leads to many miles of errors in fault location and long-term patrols for finding the fault location especially in the difficult to pass areas with bad weather. So far, a great number of fault location methods have been introduced for the transmission lines [9–30]. Some of them use the data obtained from one line terminal [9–17] and others use the data obtained from two terminals of the line [18–30]. The methods that use the data obtained from two line terminals are not dependent on the Thevenin equivalent impedance of both line sides, fault incidence angle and fault resistance; however, some of them need the synchronous data on both line sides [18–21]. Global positioning system (GPS) signal is required for data synchronization in these methods. However, when the GPS signal is lost, these methods are not useable. In order to solve this problem, a variety of methods has been introduced that use the asynchronous data of both line sides [22–30]. Some of the proposed algorithms use the lumped model of the transmission line for fault location that is not sufficiently accurate for the long lines. Therefore, some of these studies use the distributed model of the transmission line [23–27, 29]. However, these methods extract the main frequency component of the voltages and/or currents for the fault location and consequently, need a filter for separating the main component [31]. The frequency response of the filter and decaying dc component affect the accuracy of these algorithms, too. Using differential equations [32], the distributed time domain model of the transmission line is obtained which can be used to determine the location of fault [22, 33]. The distributed time domain model of transmission line fully considers the capacitance effect of the transmission line. Also, the time domain fault location method does not need to extract the main frequency component of measurements by the filter as samples in the data window during fault are taken into account. So, the distributed parameter line model in the time domain guarantees high accuracy of the fault location method.

On the other hand, employing the distributed parameter line model, the fault location problems with point of fault and synchronization time effect can be considered as a complicated optimization problem with inequality constraints that make the problem of finding the global optimum difficult utilizing any mathematical method. Thus, the PSO algorithm, considering its significant features, is employed to solve the problem.

In this paper, an accurate algorithm is presented to the fault location problem using the PSO. The distributed parameter model of the transmission line in the time domain has been utilized in the proposed method which in turn enables the algorithm to generate high accurate results. In addition, this method does not require the synchronization of the samples recorded in both line sides. For evaluating the proposed method, a 300 km/500 kV transmission line was selected, and different faults in various conditions of

[1] University of Zabol, Zabol, Electrical Engineering Department, Faculty of Engineering, Iran; E-mail: mahdi_ghazy@yahoo.com
[2] Shahid Bahonar University of Kerman, Kerman, Faculty of Technical and Engineering, Computer Engineering Department, Iran
[3] University of Zabol, Zabol, Faculty of Engineering, Electrical Engineering Department, Iran.

the system with different synchronization angles were simulated. The results showed the high accuracy of the proposed method and the lack of the dependence on the parameters of the fault and system conditions.

2. FAULT LOCATION ALGORITHM

Fig. 1 shows the single-phase model of a three-phase transmission line with the distributed parameters [32, 33]. In Fig. 1, systems A and B represent Thevenin's equivalent of the external networks. A and B denote the beginning and the end terminals of the line, and it is assumed that a fault with a resistance of R_F has occurred on the point F that is located at a distance of x from the beginning of the line. Registered samples at the beginning and at the end of the line are sent for fault locator. However, data of the beginning of the line are delivered to the fault locator with a delay of t_0 compared with the data of the end of the line, and t_0 is unknown.

In order to obtain the voltage of the fault point using the voltage and current of bus A, equation (1) can be employed [33]:

$$\begin{aligned} v_{FA}(t) = & \\ & (Z + Rx/4)^2[v_A(t + t_0 + \frac{x}{c}) \; - \\ & - (Z + Rx/4) i_A(t + t_0 + \frac{x}{c})] \\ & + (Z - Rx/4)^2[v_A(t + t_0 - \frac{x}{c}) + \\ & + (Z - Rx/4) i_A(t + t_0 - \frac{x}{c})] - \\ & - \frac{(Z + Rx/4)R}{4}[\frac{R/2}{(Z + Rx/4)} v_A(t + t_0) \; + \\ & + 2(Z - Rx/4)\, i_A(t + t_0)]/2Z^2, \end{aligned} \tag{1}$$

where

v_A, i_A – voltage and current of the bus A, respectively;

v_{FA} – voltage of the left side of the fault point;

Z – surge impedance of the line;

c – speed of the wave propagation;

R– per unit line length resistance.

Moreover, a similar equation as the equation (1) is obtained for the section FB and the right voltage of the fault v_{FB} is expressed as a function in terms of the recorded voltage and current at the end of the line (bus B) in the time domain:

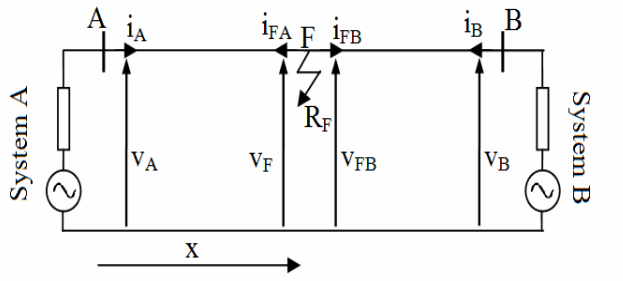

Fig. 1 – Single-phase model of a three-phase transmission line with distributed parameters.

$$\begin{aligned} v_{FB}(t) = & \\ & (Z + R(L - x)/4)^2[v_B(t + \frac{L - x}{c}) \; - \\ & - ((Z + R(L - x)/4) i_B(t + \frac{L - x}{c})] + \\ & + (Z - R(L - x)/4)^2[v_B(t - \frac{L - x}{c}) + \\ & (Z - R.(L - x)/4) i_B(t - \frac{L - x}{c})] \\ & - \frac{(Z + R(L - x)/4)R}{4}[\frac{R/2}{(\; Z + R.(L - x)/4\;)} v \\ & + 2(Z - R(L - x)/4) i_B(t) \;\;]/2Z^2, \end{aligned} \tag{2}$$

where: v_B, i_B – voltage and current of the bus B, respectively; L – length of the line from bus A to B.

Since the rupture and separation have not occurred along the line, v_{FA} and v_{FB} voltages are equal; therefore the difference between them equals to zero:

$$v_{FA} - v_{FB} = 0. \tag{3}$$

By substituting formulas (1) and (2) in (3), the following equation is achieved:

$$g(t, x, t_0) = 0. \tag{4}$$

By replacing each sample recorded during the fault occurrence in the above equation, it can be seen that this equation equals to zero only in the real place of the fault and in the accurate real time of t_0. Therefore, the following relationship is obtained by making the equation (4) discrete:

$$g(n, x, t_0) = 0, \tag{5}$$

where: $n\Delta t = t$; n – an arbitrary number; Δt – interval between two consequent samples.

Using the above formula, N equations are obtained in which there are only two unknowns of t_0 and x (N – number of the recorded samples during the fault occurrence). The following optimization problem is obtained for calculating these two unknowns using the method of least square estimation:

$$\begin{cases} \text{Min} \quad J(x, t_0) = \underset{x, t_0}{\text{Min}} \; \sum_{n=1}^{N} g^2(n, x, t_0) \\ \text{Subject to:} \quad \begin{cases} 0 < x < L \\ t_{0\text{Min}} < t_0 < t_{0\text{Max}}, \end{cases} \end{cases} \tag{6}$$

where: $t_{0\text{Min}}$, $t_{0\text{Max}}$: upper and lower limits of t_0, respectively.

Using the PSO algorithm for solving the optimization problem (6), those two unknowns (fault location and time t_0) are calculated. This formula is considered as the fitness function in the PSO algorithm which is discussed in the following section.

3. SUMMARY OF THE PSO ALGORITHM

3.1 THEORETICAL BASIS

The PSO algorithm created from observations on foraging activities of birds and their group intelligence [1].

Information is sent and contributed to other partners by a

bird while foraging for food. Consequently, according to their personal best knowledge and the swarm's best knowledge, birds maintain adjusting their path to find food for each individual. So, the bird swarms wing to a similar path. For the reason that the PSO has four features (simple idea, easy execution, robustness to control parameters, and computational efficiency), it can reach convergence quickly and achieve a good result. The PSO algorithm is employed to solve many problems such as industrial load scheduling, routing optimization, traveling salesman problem, complex non-linear optimization problems [34, 35], and low specific absorption rate path discovery in wireless body area networks [36].

3.2. PARTICLES INITIALIZATION

The PSO starts by creating a number of initial particles to be spread randomly within the solution space. Moreover, the PSO is distinguished by its capability to handle multi-variable problems for locating best result in the search space. In the PSO algorithm, each particle has its own position and velocity. Each position in the search space has a fitness quantity and represents a probable solution to the problem. Velocity stands for the speed and direction, based on which a particle modify its position in the next iteration. The mathematical symbols are as follows:

V_i^0, X_i^0 – primary velocity and position of particle i, respectively.

The following strategy is used in creating the initial place of each particle, randomly:

$$X_i^0 = (x_i^0,\ t_{0i}^0)$$

where: $x_i^0 = r_{3i}L;\ t_{0i}^0 = t_{0\text{Min}} + r_{4i}(t_{0\text{Max}} - t_{0\text{Min}});$ r_{3i}, r_{4i} – random numbers between 0 and 1, for each i.

The velocity of each particle is also determined, randomly which is similar to choosing the initial position of each particle.

The developed initialization method always guarantees to produce particles satisfying the constraints while maintaining the idea of the PSO algorithm.

3.3. FITNESS FUNCTION

A fitness function such as (6) is defined as a mathematical expression. The final goal is to obtain a point (or here a particle) which optimizes the function. By substituting a particle location into the fitness function, fitness quantity can be achieved to determine the qualities of the particle. Mathematical symbols are as follows:

J – fitness function;

$J(X_i^k)$ – fitness quantity of particle i at the k^{th} iteration, where: $X = (x, t_0)$.

3.4. VELOCITY AND LOCATION UPDATES

In the first version of PSO, each particle changes its own velocity and location according to its present velocity, the locations of the local best and global best results. The velocity that is created toward the local best and the global best locations multiplied to random numbers can identify the velocity of the particle in the next iteration:

$$V_i^{k+1} = V_i^k + c_1 r_1 (P_i^k - X_i^k) + c_2 r_2 (P_g^k - X_i^k) \tag{7}$$

$$X_i^{k+1} = X_i^k + V_i^{k+1}, \tag{8}$$

where: $k - k^{\text{th}}$ iteration;

V_i^k, X_i^k – velocity and location of particle i at the k^{th} iteration, respectively;

P_i^k – personal best location of particle i at the k^{th} iteration;

P_g^k – best location of all particles at the k^{th} iteration;

c_1, c_2 – coefficients of speeding up between 0 and 4;

r_1, r_2 – random numbers between 0 and 1.

The initial P_i^k of particle (*i.e* $k = 0$) is determined as the initial position of particle and the initial P_g^k (i.e $k = 0$) is set as the position of a particle with minimum output of (6).

Constant inertia weight [37] is an idea that a particle goes around considering a weight of velocity (w). Thus, the velocity renews as:

$$V_i^{k+1} = wV_i^k + c_1 r_1 (P_i^k - X_i^k) + c_2 r_2 (P_g^k - X_i^k) \tag{9}$$

3.5. SEARCH PROCEDURE

For the duration of the search procedure, the locations of each particle with the better fitness quantity are saved. Comparing the fitness quantity of the location reached by the particle at the $(k + 1)^{\text{th}}$ iteration with $J(P_i^k)$, the fitness quantity of the local best result is obtained. Assuming the fitness quantity of the new location is better than that of the local best result, the location reached by the particle and its fitness quantity will be utilized to renew the fitness quantity and location of the local best result. The fitness quantity of the new position reached by the particle at the $(k+1)^{\text{th}}$ iteration is compared with that of the global best result. Assuming the fitness quantity of the new location is better than that of the global best result, the location reached by the particle and its fitness quantity will be utilized to renew the fitness quantity and the location of the global best result.

3.6. STEPS FOR IMPLEMENTATION

1) Initialize particles (with random velocities V_i^0 and locations X_i^0) in the search space considering constraints.

2) Determine $J(X_i^0)$, the fitness quantity of all particles using the fitness function, and determine the local best P_i^0 and the global best P_g^0.

3) Explore in the space.

4) Renew P_i^k and P_g^k.

5) Renew the location and velocity of all particles.

6) Return to Step 3 until stopping criteria is achieved.

4. EVALUATION OF THE PROPOSED LOCATION METHOD

The proposed fault location algorithm is evaluated using the data obtained from the simulation in MATLAB/Simulink. To this end, a variety of simulations with different power system conditions has been carried out. The simulated system includes a 500 kV and 300 km transmission line. The main parameters of this power system are presented in the Appendix. For determining the accuracy of the proposed method, location error is defined based on the percentage of the line length:

$$[\%]\,\text{Error} = \frac{\text{Calculated distance} - \text{Actual distance}}{\text{Line length}} \cdot 100. \quad (10)$$

Data obtained from the simulation in MATLAB/Simulink are normally synchronous. To evaluate the proposed method, the delay time t_0 is produced for the measured voltages and currents of the bus A compared with the measured data of the bus B. Various conditions, including the various types of fault, different fault locations and different fault incidence angles have been considered in simulations. It should be noted that the minimum interval of the sampling should be more than twice the wave transmission time from the beginning to the end of the line, and samples registered in quarter of a cycle during fault were used. Meanwhile, for solving the optimization problem (6), the lower and upper limits of t_0 are respectively proportional to the –45° and 45° synchronous angle (–2038 μs and 2038 μs). In addition, to select a suitable stopping criterion which might be the maximum number of function evaluation in PSO algorithm, a variety of tests were carried out. Finally, the maximum number of 2 000 with population size of 100 resulted in accurate outcomes.

4.1. INFLUENCE OF THE FAULT TYPE AND LOCATION

The method presented in this paper is capable to find the location of the various types of the faults occurred in different points of the transmission line. Simulation studies for fault location of transmission lines undergoing various fault types are reflected in Table 1. For A-G, ABC-G, BC-G, and AC fault types (A, B, C phases, G ground), the fault resistance is considered to be 5 Ω whereas a value of 20° is considered for synchronization angle of the two-end data and the fault incidence angle is 40°. It can be observed that the fault location is highly accurate for all fault cases, and the maximum absolute error is kept below 0.07 % for the results reflected in Table 1.

4.2. INFLUENCE OF THE FAULT RESISTANCE

Fault resistance is one of the main parameters which influence on the precision of fault location methods. Thus, to evaluate the impact of fault resistance, simulations have been executed for various fault resistances (1, 10, 50 and 100 Ω) with several fault types. Simulation results are shown in Table 2. According to this table, it can be concluded that the fault locator gives an inherently high accuracy for various fault resistances.

Table 1

The error percentage of the presented technique for different fault types and locations

Fault type	Actual location of fault (km)	Calculated Synch. Angle (degree)	Calculated location of fault (km)	Error (%)
A-G	30	20.2	30.2	0.067
	90	20.2	89.9	–0.033
	160	20.2	160	0
	200	20.2	200.1	0.033
	260	20.2	259.9	–0.033
ABC-G	30	20.07	30.2	0.067
	90	20.07	89.9	–0.033
	160	20.07	160	0
	200	20.07	200.1	0.033
	260	20.07	259.9	–0.033
BC-G	30	20.2	30.2	0.067
	90	20.2	89.9	–0.033
	160	20.2	160	0
	200	20.2	200.1	0.033
	260	20.2	259.9	–0.033
AC	30	20.07	30.2	0.067
	90	20.07	89.9	–0.033
	160	20.07	160	0
	200	20.07	200.1	0.033
	260	20.07	259.9	–0.033

Table 2

The error percentage of the presented technique for different fault resistances

Fault Resistance	Actual location of fault (km)	C-G	AB-G	BC
		Fault Location Error (%)		
$R_F = 1\ \Omega$	80	–0.067	0.033	0.067
	170	0.033	0	0.033
	250	0.067	0.067	–0.033
$R_F = 10\ \Omega$	80	0	0.067	–0.067
	170	–0.033	0.033	–0.067
	250	0.067	0	0.033
$R_F = 50\ \Omega$	80	–0.033	–0.067	0.033
	170	0	–0.067	0.067
	250	–0.033	0.033	0
$R_F = 100\ \Omega$	80	0.067	–0.067	0.067
	170	0.033	0.067	–0.033
	250	0.067	0	–0.033

4.3. INFLUENCE OF THE FAULT INCIDENCE ANGLE

Fault incidence angles influence on transients of the faults. As a result, they influence on the fault location algorithms which straightly depend on the created transients.

The proposed fault location technique uses transient data, forms N equations as expressed in (5), and then minimizes the objective function which is achieved based on these equations, as in (6) using PSO algorithm. So, the accuracy of proposed technique is not corrupted by fault incidence angles, as the results in Table 3 reveal. In this table, incidence angles of 0°, 45° and 90° have been chosen to demonstrate the results of the fault location while the fault resistance is set to 2 Ω, and the synchronization angle is considered to be –20°. As Table 3 demonstrates, there is no incidence angle for which the proposed scheme is unsuccessful to locate the fault. Also, the maximum absolute error is 0.067 % which is definitely acceptable.

Table 3

The error percentage of the presented technique for different fault incidence angles

Fault type	Actual location of fault (km)	Incidence angle=0°	Incidence angle=45°	Incidence angle=90°
		Fault location error (%)		
B-G	35	0.033	0.033	0.033
	95	–0.067	–0.067	–0.067
	165	0	0	0
	205	–0.033	–0.033	–0.033
	265	0	0	0
AC-G	35	0.033	0.033	0.033
	95	–0.067	–0.067	–0.067
	165	0	0	0
	205	–0.033	–0.033	–0.033
	265	0	0	0
AB	35	0.033	0.033	0.033
	95	–0.067	–0.067	–0.067
	165	0	0	0
	205	–0.033	–0.033	–0.033
	265	0	0	0

4.4. INFLUENCE OF THE SYNCHRONIZATION ANGLES

To further analyze the scheme, different synchronization angles have been added to the recorded data at terminal A compared to the recorded data at terminal B obtained from MATLAB/Simulink. Table 4 shows the fault location results for different synchronization angles (SAs) and various fault types with 30° incidence angle and 5 Ω fault resistance happening at different distances from terminal A. As it can be seen from this table, the maximum absolute error is 0.067 %.

Table 4

The error percentage of the presented technique for different synchronization angles

Fault type	Actual location of fault (km)	SA= –25°	SA = –13°	SA= 15°	SA= 27°
		Fault Location Error (%)			
C-G	20	0.067	–0.033	0.033	0.067
	110	0.067	0	0.033	0.067
	220	0	0.2	0	0
	270	0.033	–0.033	–0.067	0.033
ABC-G	20	0.067	–0.033	0.033	0.067
	110	0.067	0	0.033	0.067
	220	0	0.067	0	0
	270	0.033	–0.033	–0.067	0.033
AB-G	20	0.067	–0.033	0.067	–0.067
	110	–0.033	0.067	0	–0.067
	220	0.067	0.067	0.067	0.067
	270	0.033	0.033	0.033	–0.033
BC	20	0.067	–0.033	0.067	–0.067
	110	–0.033	0.067	0	–0.067
	220	0.067	0.067	0.067	0.067
	270	0.033	0.033	0.033	–0.033

4.5. **INFLUENCE OF SOURCE IMPEDANCE VARIATION**

Since power system is a dynamic system, changing the source impedance ratio (SIR), may affect sensitivity, selectivity and accuracy of the protection system [38].

For investigating the impact of source impedance variation on the accuracy of the presented technique, source impedance at terminal A, terminal B or both of them have been varied. Fault location results for B-G fault occurring at five distances (25, 105, 185, 235, and 285 km from terminal A) with –15° synchronization angle and fault resistance of 10 Ω have been shown in Table 5. As observed in this table, source impedance changes have an insignificant impact on the fault location precision. This was probable since the presented method is independent of the source impedances when the fault location equations and optimization problem are derived.

The fault-location errors presented in this paper have been compared with the existing study in [25–27]. The maximum fault location errors reported in [25–27] is 0.2 %, 0.12 %, and 0.15 % respectively, whereas in the presented study, as concluded from Tables 1–5, the maximum absolute of the fault location error is 0.067 %.

5. **CONCLUSION**

This paper proposes a PSO-based fault location method when unsynchronized measurements are available from two sides of the line. Shunt capacitance effect of the transmission lines is fully considered employing the distributed time-domain model of the transmission line. As a result, higher precision is obtained for the presented algorithm compared to the previously published papers. In order to confirm the efficiency of the method, validation tests have been utilized which verify the high accuracy of the proposed technique such that the maximum absolute of the fault location errors has been kept below 0.07 % of the line length. Sensitivity tests have also been carried out to study the effects of fault‘s type, resistance and inception angle, as well as the sources’ impedances and data synchronization angle at the terminals, which demonstrate that the location accuracy is not affected by these parameters.

Table 5

The error percentage of the presented technique for various source impedances

Source impedance variation	Actual location of fault (km)	Calculated location of fault (km)	Error (%)
+50% at A Terminal	25	25.2	0.067
	105	105	0
	185	184.9	–0.033
	235	235.1	0.033
	285	285.2	0.067
+50% at B Terminal	25	25.2	0.067
	105	105	0
	185	184.9	–0.033
	235	235.1	0.033
	285	285.2	0.067
+50% at A Terminal and +50% at B Terminal	25	25.2	0.067
	105	105	0
	185	184.9	–0.033
	235	235.1	0.033
	285	285.2	0.067

APPENDICES

Power system:

Nominal voltage of power system: 500 kV
Nominal frequency of power system: 60 Hz
Phase angle between voltage sources: 20°

Transmission line:

Zero-sequence:
R_0= 0.275 Ω/km, L_0= 3.4505998 mH/km, C_0= 8.5 nF/km
Positive- and negative-sequence:
R_1= 0.0275 Ω/km, L_1=1.002768 mH/km, C_1=13 nF/km.

Received on March 16, 2016

REFERENCES

1. J. Kennedy, R. Eberhart, *Particle swarm optimization*, Proceedings IEEE International Conference on Neural Networks (ICNN'95), Perth, Australia, Piscataway, NJ, USA, IEEE, Nov/Dec 1995, pp. 1942–1948.
2. H. Yoshida, K. Kawata, Y. Fukuyama, S. Takayama, Y. Nakanishi, *A particle swarm optimization for reactive power and voltage control considering voltage security assessment*, IEEE Trans. Power Syst., **15**, pp. 1232–1239 (2000).
3. M. Clerc, J. Kennedy, *The particle swarm-explosion, stability, and convergence in a multidimensional complex space*, IEEE Trans. Evol. Comput., **6**, *1*, pp. 58–73 (2002).
4. J.-B. Park, K.-S. Lee, J-R Shin, K.Y. Lee, *A particle swarm optimization for economic dispatch with nonsmooth cost functions*, IEEE Trans. Power Syst., **20**, *1*, pp. 34–42 (2005).
5. M.A. Abido, *Optimal design of power-system stabilizers using particle swarm optimization*, IEEE Trans. Energy Conv., **17**, *3*, pp. 406–413 (2002).
6. I.N. Kassabalidis, M.A. El-Sharkawi, R.J. Marks, L.S. Moulin, A.P.A. da Silva, *Dynamic security border identification using enhanced particle swarm optimization*, IEEE Trans. Power Syst., **17**, pp. 723–729 (2002).
7. M. Sreejeth, M. Singh, P. Kumar, *Particle swarm optimization in efficiency improvement of vector controlled surface mounted permanent magnet synchronous motor drive*, IET Power Electron., **8**, pp. 760–769 (2015).
8. M. Khiat, A. Marano, S. Chettih, J.L.M. Ramos, *A hybrid methodology for optimal VAR dispatch in the western Algerian power system*, Rev. Roum. Sci. Techn. – Électrotechn. et Énerg., **57**, *4*, pp. 361–370 (2012).
9. C.E.M. Pereira, Jr.L.C. Zanetta, *Fault location in transmission lines using one-terminal post-fault voltage data*, IEEE Trans. Power Del., **19**, *2*, pp. 570–575 (2004).
10. Q. Zhang, Y. Zhang, W. Song, Y. Yu, *Transmission line fault location for phase-to-earth fault using one-terminal data*, IEE Proc – Gener Transm Distrib., **146**, *2*, pp. 121–124 (1999).
11. T. Takagi, Y. Yamakoshi, M. Yamaura, R. Kondou, T. Matsushima, *Development of a new type fault locator using the one terminal voltage and current data*, IEEE Transactions, PAS-**101**, **8**, pp. 2892–2898 (1982).
12. J. Sadeh, A.M. Ranjbar, N. Hadjsaid, R. Feuillet, *Accurate fault location algorithm for power transmission lines*, ETEP, **10**, *5*, pp. 313–318 (2000).
13. O.A.S. Youssef, *A new technique for location of transmission line faults using single-terminal voltage and current data*, Electric Power Systems Research, **23**, pp. 123–128 (1992).
14. Z.M. Radojevic, V.V. Terzija, M.B. Djuric, *Multipurpose overhead lines protection algorithm*, IEE Proc. Generation, Transmission and Distribution, **146**, *5*, pp. 441–445 (1999).
15. T. Adu, A new transmission line fault locating system, IEEE Trans. Power Del., **16**, *4* (2001).
16. H.-X. Ha, B.-H. Zhang, Z.-L. Lv, *A novel principle of single-ended fault location technique for EHV transmission lines*, IEEE Trans. Power Del., **18**, *4* (2003).
17. J. Suonan, J. Qi, *An accurate fault location algorithm for transmission line based on R–L model parameter identification*, Electric Power Systems Research, **76**, pp. 17–24 (2005).
18. M. Kezunovic´, J. Mrkic´, B. Perunicic´, *An accurate fault location algorithm using synchronized sampling*, Electric Power Systems Research, **29**, pp. 161–169 (1994).
19. S.M. Brahma, A.A. Girgis, *Fault location on a transmission line using synchronized voltage measurements*, IEEE Trans. Power Del., **19**, *4*, pp. 1619–1622 (2004).
20. J.A. Jiang, J.Z. Yang, Y.H. Lin, C.W. Liu, J.C. Ma, *An adaptive PMU based fault detection/location technique for transmission lines-part I: theory and algorithms*, IEEE Trans. Power Del., **15**, *2*, pp. 486–493 (2000).
21. J.A. Jiang, Y.H. Lin, J.Z. Yang, T.M. Too, C.W. Liu, *An adaptive PMU based fault detection/location technique for transmission lines-part II: PMU implementation and performance evaluation*, IEEE Trans. Power Del., **15**, *4*, pp. 1136–1146 (2000).
22. M. Ghazizadeh-Ahsaee, *Accurate NHIF locator utilizing two-end unsynchronized measurements*, IEEE Trans. Power Del., **28**, *1*, pp. 419–426 (2013).
23. A.A. Girgis, D.G. Hart, W.L. Peterson, *A new fault location technique for two and three-terminal lines*, IEEE Trans. Power Del., **7**, *1*, pp. 98–107 (1992).
24. Y. Liao, *Unsynchronized fault location based on distributed parameter line model*, Electric Power Components and Systems, Sep. 2007, pp. 1061–1077.
25. Y. Liao, *Fault location utilizing unsynchronized voltage measurements during fault*, Electric Power Components and Systems, 2006, pp. 1283–1293.
26. J. Izykowski, R. Molag, E. Rosolowski, M. Saha, *Accurate location of faults on power transmission lines with use of two-end unsynchronized measurements*, IEEE Trans. Power Del., **21**, *2*, pp. 627–633 (2006).
27. J. Izykowski, E. Rosolowski, P. Balcerek, M. Fulczyk, M.M. Saha, *Accurate noniterative fault-location algorithm utilizing two-end unsynchronized measurements*, IEEE Trans. Power Del., **25**, *1*, pp. 72–80 (2010).
28. D. Novosel, D.G. Hart, E. Udren, J. Garitty, *Unsynchronized two-terminal fault location estimation*, IEEE Trans. Power Del., **11**, *1*, pp. 130–138 (1996).
29. A.L. Dalcastagne, S.N. Filho, H.H. Zurn , R. Seara, *An iterative two-terminal fault-location method based on unsynchronized phasors*, IEEE Trans. Power Del., **23**, *4*, pp. 2318–2329 (2008).
30. E.G. Silveira, C. Pereira, *Transmission line fault location using two-terminal data without time synchronization*, IEEE Trans. Power Syst., **22**, *1*, pp. 498–499 (2007).
31. M. Istrate, M. Guşa, *Assessment of two single-end fault location algorithms in an ATP approach,* Rev. Roum. Sci. Techn. – Électrotechn. et Énerg., **54**, *4*, pp. 345–354 (2009).
32. H. Dommel, *Digital computer solution of electromagnetic transient in single and multi-phase networks*, IEEE Trans. Power Apparatus and Systems, PAS-**98**, *4*, pp. 388–399 (1969).
33. M. Ghazizadeh-Ahsaee, *Fault location for long transmission lines utilizing two-end unsynchronized data in the time domain*, (in Persian), 27th Int. Power System Conf. (PSC 2012), Tehran, Iran, Nov. 2012.
34. G. Alizadeh, M. Baradarannia, P. Yazdizadeh, Y. Alipouri, *Serial configuration of genetic algorithm and particle swarm optimization to increase the convergence speed and accuracy*, Proc. 10th Int. Conf. Intell. Syst. Design Appl. (ISDA), Nov./Dec. 2010, pp. 272–277.
35. G. Zhang, M. Dou, S. Wang, *Hybrid genetic algorithm with particle swarm optimization technique*, Proc. Int. Conf. Comput. Intell. Secur. (CIS), Dec. 2009, pp. 103–106.
36. T.-Y. Wu, Ch.-H. Lin, *Low-SAR path discovery by particle swarm optimization algorithm in wireless body area networks*, IEEE Sens. J., **15**, pp. 928–936 (2015).
37. Y. Shi, R. Eberhart, *A modified particle swarm optimizer*, Proc. IEEE Int. Conf. Evol. Comput., pp. 69–73, May 1998.
38. I.C. Borascu, *Proposal of an adaptive overcurrent relay for 110 KV network*, Rev. Roum. Sci. Techn. – Électrotechn. et Énerg., **60**, *4*, pp. 376–386 (2015).